# Analysis of Crosstie Track in Lateral Plane Using New Track Equations

By Harry W. Shenton III,[1] Associate Member, ASCE

(Reviewed by the Urban Transportation Division)

**Abstract:** The analysis of a crosstie railroad track in the lateral plane has traditionally been based on the theory of a beam on an elastic foundation, in which the bending rigidity of the track structure is assumed to be twice the rigidity of a single rail, and the ballast resistance is represented by a linear Winkler foundation with modulus $k$. The traditional analysis ignores the contribution of the ties and rail-tie fasteners to the bending stiffness of the track and the nonlinearity of the ballast resistance. In the present paper the analysis of an infinitely long crosstie track subject to a concentrated lateral load is presented. The analysis is based on the new track equations derived by Kerr and Zarembski in 1981. These equations explicitly account for the contribution of the rails, ties, and fasteners to the bending stiffness of the track. A bilinear approximation is assumed in modeling the lateral resistance due to the ballast. A closed form solution for the track deflection is obtained using the new equations, for displacements in the linear regime. A closed-form solution is obtained for the nonlinear response, using a simplified set of track equations. A method for determining the model track parameters is presented that is based on a least-squares fit to experimental load-deflection data. Results show that the analytical solution accurately predicts the measured data, for the full range of loads and over the entire length of the track.



## INTRODUCTION

The stress and deformation of a crosstie railroad track in the lateral plane has traditionally been calculated using the theory of a beam on an elastic foundation, in which the lateral bending rigidity of the track structure is assumed to be twice the rigidity of a single rail. Also, the resistance provided by the ballast is assumed to be linearly related to the track deflection. This analysis neglects the contribution of the ties and rail-tie fasteners to the bending stiffness of the track; furthermore, experiments suggest that the lateral resistance provided by the ballast is highly nonlinear (Fig. 1). To overcome some of these limitations, complex finite-element analyses have been conducted that take into account these and other effects (Arbabi and Li 1988), while others have proposed nonlinear models for the ballast resistance. Many of these approaches are either too time consuming and complex for routine design analyses, or they neglect the significant contribution of some of the track components just mentioned.

Kerr and Zarembski (1981a) systematically derived a set of three differential equations for the analysis of a crosstie railroad track in the lateral plane; subsequently, the equations were generalized by Kerr and Accorsi (1985) for the analysis of frame-type structures. The analytical model of the track is shown in Fig. 2. The derivation used the fact that the track consists of a series of repetitive units; therefore, the stiffness of any one interior joint is identical to the stiffness of another. Based on this, equations of equilibrium were derived for any arbitrary joint using slope-deflection equations. Difference equations were then written for adjacent joints and differential equations were derived in a limiting process, in which the tie spacing tends to zero. The resulting equations have well-defined coefficients in terms of the flexural rigidity of the rails and ties, torsional resistance of the rail-tie fasteners, distance between the rails, and the center-to-center tie spacing. The equations have been validated experimentally and analytically, for the track-structure without ballast, for static load by Kerr and Zarembski (1981b) and by Kerr and Accorsi (1987), and for the dynamic case by Kerr and El-Sibaie (1987a,b). A simplified version of the equations has also been studied that are easier to solve, yet still retain the explicit functionality of the various track components. The simplified equations have been shown to be accurate, for the track structure without ballast, for a wide range of track parameters (Kerr, unpublished report, 1984).

The purpose of this paper is to present the analysis of a crosstie track using the new track equations and a nonlinear model for the ballast resistance. The analysis is for an infinitely long track embedded in ballast, subject to a concentrated lateral load. A bilinear approximation is assumed for the lateral resistance due to the ballast, as shown in Fig. 3, in which

$$\rho(x) = k\hat{v}(x) \quad \text{for } \hat{v} < \hat{v}^* \qquad \rho(x) = \rho_0 = k\hat{v}^* = \text{constant} \quad \text{for } \hat{v} > \hat{v}^* \tag{1}$$

where $\rho(x)$ = ballast resistance; $k$ = initial linear stiffness; $\rho_0$ = constant resistance; $\hat{v}(x)$ = lateral track deflection; and $\hat{v}^*$ =

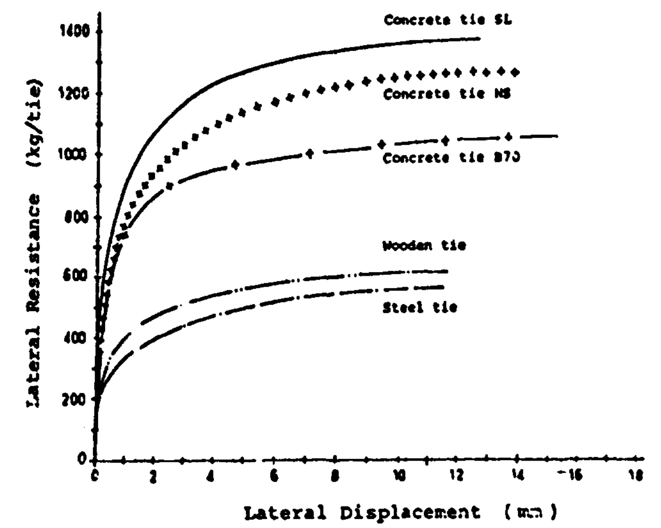


**FIG. 1. Ballast Resistance versus Lateral Displacement (Dogneton 1978)**

[1]Asst. Prof., Dept. of Civ. and Envir. Engrg., Univ. of Delaware, Newark, DE 19716.

Note. Discussion open until November 1, 1997. To extend the closing date one month, a written request must be filed with the ASCE Manager of Journals. The manuscript for this paper was submitted for review and possible publication on August 7, 1996. This paper is part of the ***Journal of Transportation Engineering***, Vol. 123, No. 3, May/June, 1997. ©ASCE, ISSN 0733-947X/97/0003-0202–0208/$4.00 + $.50 per page. Paper No. 13915.



J. Transp. Eng., 1997, 123(3): 202-208

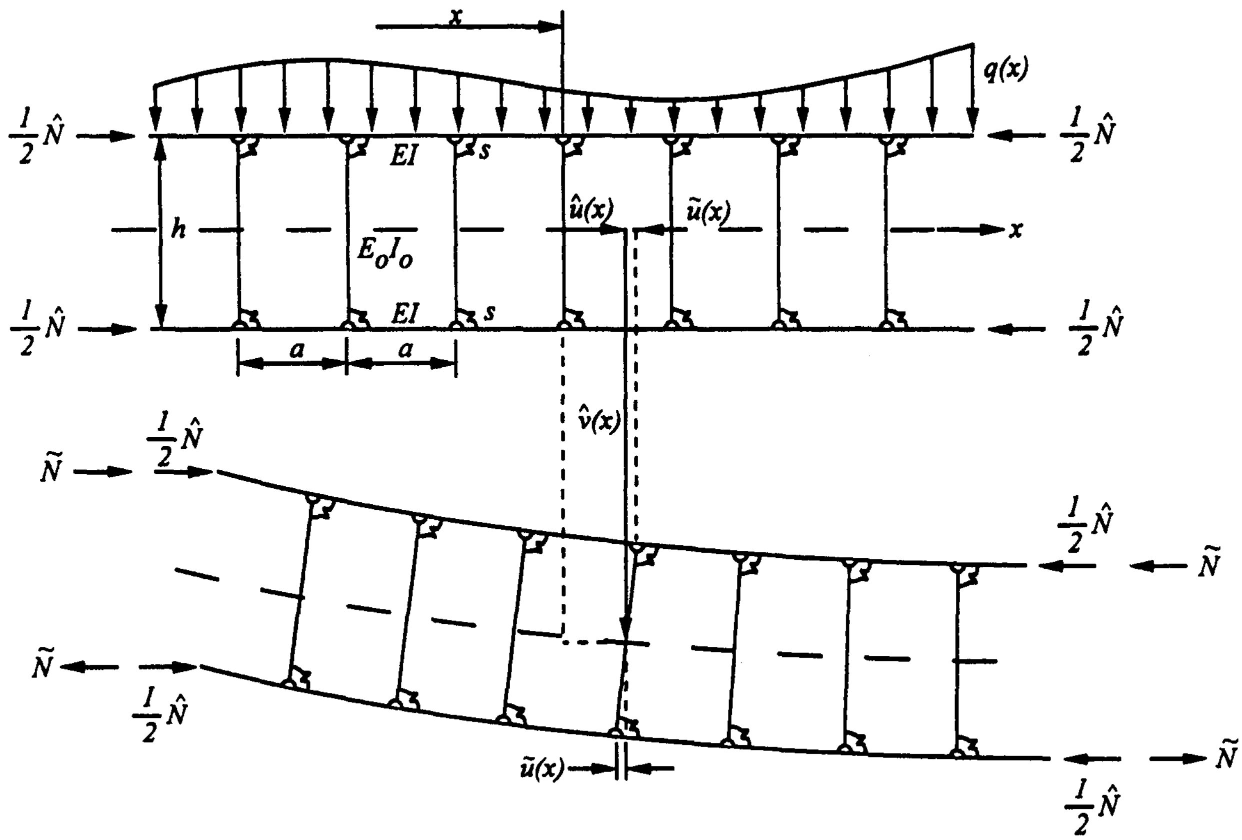


FIG. 2. Analytical Model of Crosstie Track

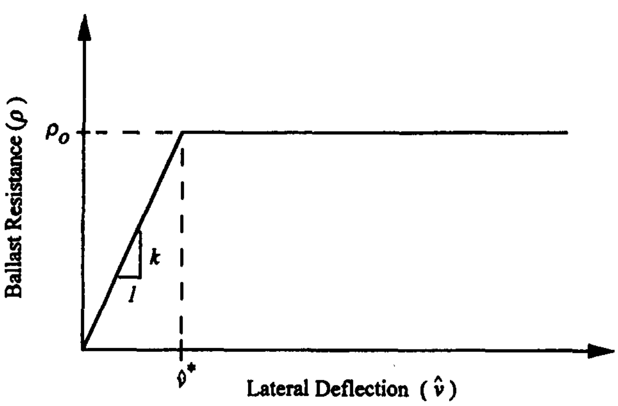


FIG. 3. Bilinear Approximation for Ballast Resistance

critical deflection that defines the transition point as shown in Fig. 3. The exact and simplified new track equations are solved in closed-form, assuming a linear foundation response (i.e., for $\hat{v} < \hat{v}^*$). Results of the two analyses are compared for a range of realistic track parameters and shown to be in good agreement. The simplified equations are then solved for $\hat{v} > \hat{v}^*$. Closed-form expressions are obtained for the track deflections and bending moments, that are suitable for routine design and analysis. Finally, a method for determining the necessary track parameters from recorded test data is presented.

## NEW TRACK EQUATIONS

The differential equations governing the response of the track beam, shown in Fig. 2, as derived by Kerr and Zarembski (1981a) are

$$2EI\frac{d^4\hat{v}}{dx^4} + (\hat{N} - \kappa)\frac{d^2\hat{v}}{dx^2} + \frac{2\kappa}{h}\frac{d\tilde{u}}{dx} = q \qquad (2)$$

$$EA\frac{d^2\tilde{u}}{dx^2} - \frac{2\kappa}{h^2}\tilde{u} + \frac{\kappa}{h}\frac{d\hat{v}}{dx} = 0; \quad 2EA\frac{d^2\hat{u}}{dx^2} = 0 \qquad (3, 4)$$

where

$$\kappa = \frac{12K^*s^*}{6K^* + s^*}; \quad s^* = \frac{s}{a}; \quad K^* = \frac{E_0I_0}{ah} \qquad (5)$$

In the preceding equations, $\hat{v}(x)$ and $\hat{u}(x)$ = lateral and axial displacement of the track axis, respectively; $\tilde{u}(x)$ = axial displacement of an individual rail due to lateral bending; $E$ = Young's modulus of the rail steel; $I$ = moment of inertia of one rail with respect to its vertical centroidal axis; $A$ = cross-sectional area of one rail; $E_0$ = Young's modulus of the tie; $I_0$ = moment of inertia of the tie with respect to its vertical centroidal axis; $s$ = rotational stiffness of one rail-tie fastener; $a$ = tie spacing; and $h$ = track gauge. The internal member forces for the track structure are

$$\hat{N} = -2EA\frac{d\hat{u}}{dx}; \quad \tilde{N} = -EA\frac{d\tilde{u}}{dx}; \quad \hat{M} = M_b + \tilde{M} \qquad (6–8)$$

$$M_b = -2EI\frac{d^2\hat{v}}{dx^2}; \quad \tilde{M} = -hEA\frac{d\tilde{u}}{dx} \qquad (9, 10)$$

$$\hat{V} = -2EI\frac{d^3\hat{v}}{dx^3} - (\hat{N} - \kappa)\frac{d\hat{v}}{dx} - \frac{2\kappa}{h}\tilde{u} \qquad (11)$$

where $\hat{N}$ = axial force of the track beam; $\tilde{N}$ = axial force in a rail due to lateral bending; $\hat{M}$ = total bending moment of the track beam; $M_b$ = bending moment in two rails; $\tilde{M}$ = bending moment due to $\tilde{N}$; and $\hat{V}$ = shear force in two rails.

## FORMULATION AND SOLUTION FOR $\hat{v} < \hat{v}^*$ USING NEW TRACK EQUATIONS

Consider the problem of an infinitely long crosstie track embedded in ballast and subject to a concentrated lateral load

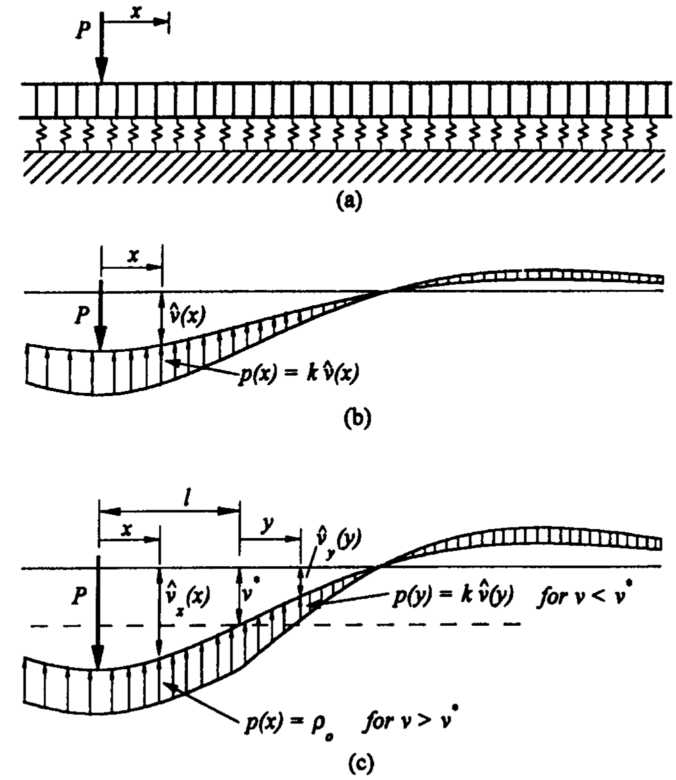


**FIG. 4. Definition Diagram**

$P$ [Fig. 4(a)]. The origin of the coordinate system is placed at the load, with positive $x$ to the right. According to the bilinear approximation, for $\hat{v} < \hat{v}^*$, the resistance exerted by the ballast on the track structure is represented by a Winkler foundation with track modulus $k$ [Fig. 4(b)]. Assuming $\hat{N} \equiv 0$ and noting that $q \equiv 0$, (2) and (3) reduce to

$$2EI\hat{v}'''' - \kappa\hat{v}'' + \frac{2\kappa}{h}\bar{u}' + k\hat{v} = 0 \tag{12}$$

$$EA\bar{u}'' - \frac{2\kappa}{h^2}\bar{u} + \frac{\kappa}{h}\hat{v}' = 0 \tag{13}$$

in which ( )$' = d/dx$. The necessary boundary conditions are

$$\hat{v}'(0) = 0; \quad \hat{v}'''(0) = \frac{P}{4EI} \tag{14, 15}$$

$$\bar{u}(0) = 0; \quad \lim_{x\to\infty} \{\hat{v}, \hat{v}', \bar{u}\} \to \text{finite} \tag{16, 17}$$

Eqs. (12) and (13) are coupled ordinary differential equations with constant coefficients. The two equations can be uncoupled as follows; solving (12) for $\bar{u}'$ yields

$$\bar{u}' = \frac{-EIh}{\kappa}\hat{v}'''' + \frac{h}{2}\hat{v}'' - \frac{kh}{2\kappa}\hat{v} \tag{18}$$

Differentiating (13) once yields

$$EA\bar{u}''' - \frac{2\kappa}{h^2}\bar{u}' + \frac{\kappa}{h}\hat{v}'' = 0 \tag{19}$$

Differentiating (18) twice with respect to $x$ and substituting that and (18) into (19) yields a single sixth-order equation for the lateral deflection of the track beam

$$\hat{v}^{vi} - \beta^2\hat{v}'''' + \alpha\hat{v}'' - \gamma\hat{v} = 0 \tag{20}$$

in which

$$\beta^2 = \frac{\kappa}{2EI}\left(1 + \frac{4I}{Ah^2}\right); \quad \alpha = \frac{k}{2EI}; \quad \gamma = \frac{\kappa k}{E^2IAh^2} \tag{21}$$

In a similar manner, boundary condition (16) is expressed in terms of $\hat{v}$ as

$$\hat{v}^{v}(0) = \frac{P\kappa}{8(EI)^2} \tag{22}$$

The solution to (20) is obtained by assuming $\hat{v}(x) = e^{mx}$, which yields the characteristic equation

$$m^6 - \beta^2m^4 + \alpha m^2 - \gamma = 0 \tag{23}$$

Setting $n = m^2$ yields

$$n^3 - \beta^2n^2 + \alpha n - \gamma = 0 \tag{24}$$

The nature of the roots of (24) are governed by the function (Beyer 1981)

$$C = \frac{1}{27}\{4\alpha^3 + 27\gamma^2 + 4\beta^6\gamma - \beta^4\alpha^2 - 18\beta^2\alpha\gamma\} \tag{25}$$

which can be positive, negative, or zero, depending on the value of the track parameters. When $C$ is positive, there is one real root and a pair of complex conjugate roots, and the resulting solution for the track deformation is in the form of a decaying harmonic, which is similar in form to the traditional analysis. In this case, the roots of (24) can be expressed as

$$n_1 = -(R_1 + R_2) + \frac{\beta^2}{3} \tag{26}$$

$$n_{2,3} = \frac{R_1 + R_2}{2} + \frac{\beta^2}{3} \pm i\frac{\sqrt{3}}{2}(R_1 - R_2) \tag{27}$$

in which

$$R_1 = \sqrt[3]{\frac{Q + \sqrt{C}}{2}}; \quad R_2 = \sqrt[3]{\frac{Q - \sqrt{C}}{2}}; \quad Q = \frac{-2\beta^6}{27} + \frac{\beta^2\alpha}{3} - \gamma \tag{28}$$

It follows that the roots of (23) can be expressed as

$$m_{1,2} = \pm\sqrt{n_1} = \pm\zeta \tag{29}$$

$$m_{3,4} = \pm\sqrt{n_2} = \pm(\xi + i\eta) \tag{30}$$

$$m_{5,6} = \pm\sqrt{n_3} = \pm(\xi - i\eta) \tag{31}$$

in which

$$\zeta = \sqrt{-(R_1 + R_2) + \frac{\beta^2}{3}} \tag{32}$$

$$\xi = \frac{\sqrt{3/8}(R_1 - R_2)}{\sqrt{-\frac{1}{2}(R_1 + R_2) - \frac{\beta^2}{3} + \sqrt{R_1^2 - R_1R_2 + R_2^2 + \frac{\beta^2}{3}(R_1 + R_2) + \frac{\beta^4}{9}}}} \tag{33}$$

$$\eta = \frac{1}{\sqrt{2}}\sqrt{-\frac{1}{2}(R_1 + R_2) - \frac{\beta^2}{3} + \sqrt{R_1^2 - R_1R_2 + R_2^2 + \frac{\beta^2}{3}(R_1 + R_2) + \frac{\beta^4}{9}}} \tag{34}$$

With the roots evaluated, the general solution to (20) can be written as

$$\hat{v}(x) = a_1e^{\zeta x} + a_2e^{-\zeta x} + e^{\xi x}(a_3\cos\eta x + a_4\sin\eta x) + e^{-\xi x}(a_5\cos\eta x + a_6\sin\eta x) \tag{35}$$

Finally, substituting (35) into boundary conditions (14), (15), (17), and (22) yields for the six unknown coefficients

$$a_2 = \frac{-P}{8EI\zeta}\frac{[4(\xi^2 + \eta^2) - 2\bar{\beta}^2]}{[2\zeta^2(\xi^2 + \eta^2) - (\xi^2 + \eta^2)^2 - \zeta^4]} \tag{36}$$



J. Transp. Eng., 1997, 123(3): 202-208

$$a_5 = \frac{P}{8EI\xi} \frac{[(\eta^4 - 10\xi^2\eta^2 + 5\xi^4) - \zeta^4 + \bar{\beta}^2(\zeta^2 - 3\xi^2 + \eta^2)]}{(\xi^2 + \eta^2)[2\zeta^2(\xi^2 + \eta^2) - (\xi^2 + \eta^2)^2 - \zeta^4]} \quad (37)$$

$$a_6 = \frac{P}{8EI\eta} \frac{[(\xi^4 - 10\xi^2\eta^2 + 5\eta^4) - \zeta^4 + \bar{\beta}^2(\zeta^2 + 3\eta^2 - \xi^2)]}{(\xi^2 + \eta^2)[2\zeta^2(\xi^2 + \eta^2) - (\xi^2 + \eta^2)^2 - \zeta^4]} \quad (38)$$

and $a_1 = a_3 = a_4 = 0$, and where

$$\bar{\beta} = \frac{\kappa}{2EI} \quad (39)$$

Eq. (35) could be compared to the traditional analysis which assumes the bending rigidity is twice the rigidity of a single rail. In this case, however, the equations for the track deflection and internal member forces are explicit functions of the geometric and material properties of the rails, ties, fasteners and ballast. Note that the axial deformation of the track, $\bar{u}$, can also be obtained by substituting the solution for $\hat{v}(x)$ into (18) and integrating.

The maximum track deflection, at $x = 0$, is given by

$$\hat{v}_{max} = a_2 + a_5 \quad (40)$$

and the maximum bending moment in the two rails, at $x = 0$, is given by

$$M_b(0) = -2EI(\zeta^2 a_2 + (\xi^2 - \eta^2)a_5 - 2\xi\eta a_6) \quad (41)$$

Using (40) and (41), parametric studies may be conducted to determine the effect of varying track parameters on the response of the track.

## SIMPLIFIED TRACK EQUATIONS

The new track equations [(2) and (3)] are coupled through the term $-2\bar{u}/h + \hat{v}'$, and its derivative, which represents the angle through which the crossties rotate in the horizontal plane as the track deforms laterally. The exact equations can be uncoupled, as illustrated in the previous section; however, the resulting equation is of higher order, thus making a closed-form solution for the nonlinear foundation response ($\hat{v} > \hat{v}^*$) nearly intractable. However, if it is assumed that

$$\frac{2\bar{u}}{h} << \hat{v}' \quad (42)$$

then the new track equations become

$$2EI\hat{v}'''' + (\hat{N} - \kappa)\hat{v}'' = q(x); \quad EA\bar{u}'' + \frac{\kappa}{h}\hat{v}' = 0 \quad (43, 44)$$

The simplified track equations [(43) and (44)] were found to be valid for static loading of the track structure without ballast, if $4I/Ah^2 << 1$ (Kerr and Accorsi 1987), which is generally the case for most cross-tie tracks (e.g., $4I/Ah^2 = 0.001 << 1$, for a track with UIC rail and standard wooden ties). Note that (43) and (44) are uncoupled, yet the equations still retain the explicit functionality of the various track parameters.

The simplified expressions for the internal forces are as given in (6)–(11), with the exception that the shear force is

$$\hat{V} = -2EI\hat{v}''' - (\hat{N} - \kappa)\hat{v}' \quad (45)$$

## FORMULATION AND SOLUTION FOR $\hat{v} < \hat{v}^*$ USING SIMPLIFIED EQUATIONS

An analysis of the track structure is conducted, as in the previous section for $\hat{v} < \hat{v}^*$, using the simplified equations and the ballast represented by a Winkler foundation with modulus $k$. The governing equation for $\hat{v}$ can be expressed as

$$\hat{v}'''' - \bar{\beta}^2\hat{v}'' + \alpha\hat{v} = 0 \quad (46)$$

in which $\alpha$ and $\bar{\beta}^2$ are given in (21) and (39), respectively. The necessary boundary conditions are

$$\hat{v}'(0) = 0; \quad \hat{v}'''(0) = \frac{P}{4EI}; \quad \lim_{x\to\infty} \{\hat{v}, \hat{v}'\} \to \text{finite} \quad (47–49)$$

The general solution to (46) is

$$\hat{v}(x) = e^{-\xi x}(a_1 \cos \eta x + a_2 \sin \eta x) + e^{\xi x}(a_3 \cos \eta x + a_4 \sin \eta x) \quad (50)$$

in which

$$\xi = \frac{1}{2}\sqrt{4\lambda^2 + \bar{\beta}^2}; \quad \eta = \frac{1}{2}\sqrt{4\lambda^2 - \bar{\beta}^2}; \quad \lambda^4 = \frac{\alpha}{4} = \frac{k}{8EI} \quad (51)$$

provided $\alpha > \bar{\beta}^2/4$, or $k > \kappa^2/(8EI)$.

Substituting (50) into boundary conditions (47) through (49) yields

$$a_1 = \frac{P}{8EI}\frac{1}{\xi(\xi^2 + \eta^2)}; \quad a_2 = \frac{P}{8EI}\frac{1}{\eta(\xi^2 + \eta^2)} \quad (52)$$

and $a_3 = a_4 = 0$. The resulting equation for the track deflection is

$$\hat{v}(x) = \frac{P}{8EI\xi\eta(\xi^2 + \eta^2)} e^{-\xi x}(\eta \cos \eta x + \xi \sin \eta x) \quad (53)$$

The accuracy of the simplified equation can be established by comparing the simplified and exact solutions for a typical track. The deflection at $x = 0$, as predicted by the simplified and exact equations [(40) and (53)], is presented in Fig. 5, for varying $k$ and three values of $s$. These results correspond to a track with $E = 206 \times 10^6$ kN/m$^2$ ($30 \times 10^3$ ksi); $I = 5.13 \times 10^{-6}$ m$^4$ (12.32 in.$^4$); $E_0 = 9.8 \times 10^6$ kN/m$^2$ ($1.42 \times 10^3$ ksi), $I_0 = 2.35 \times 10^{-4}$ m$^4$ (565 in.$^4$), $A = 7.686 \times 10^{-3}$ m$^2$ (11.91 in.$^2$), $a = 0.5$ m (19.5 in.), and $h = 1.51$ m (59.4 in.). Note for this case $4I/Ah^2 = 0.00117$. In these figures the solid line corresponds to the solution of the exact equations, the circular points correspond to the simplified equations. Note that the results are indistinguishable for the range of $k$ [2,000–12,000 kN/m$^2$ (0.3–1.7 ksi)] and $s$ [100–2,000 kN-m/rad (900–18,000 kip-in./rad)] studied.

## FORMULATION AND SOLUTION FOR $\hat{v} > \hat{v}^*$ USING SIMPLIFIED EQUATIONS

According to the bilinear approximation, the track deflects laterally under a linearly increasing lateral resistance until it

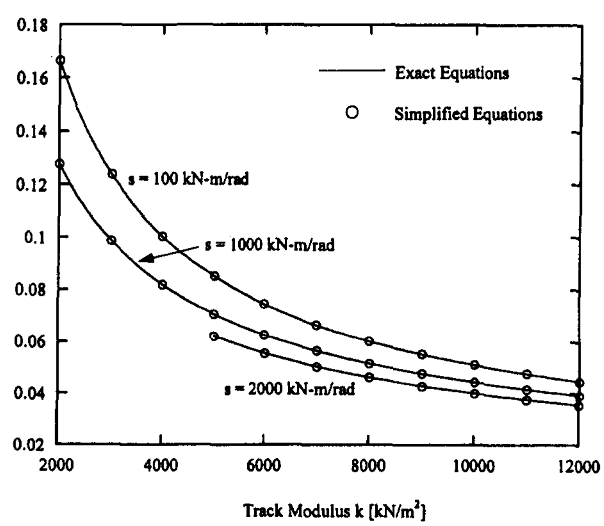


**FIG. 5. Comparison of Deflection at $x = 0$ from Simplified and Exact Solutions**





J. Transp. Eng., 1997, 123(3): 202-208

reaches a maximum constant value $\rho_0$. Referring to (53), this occurs when $\hat{v}(0) = \hat{v}^* = P/8EI\xi(\xi^2 + \eta^2) = P\lambda^2/2k\xi$, i.e., when the load reaches

$$P^* = \frac{2k\xi\hat{v}^*}{\lambda^2} \quad (54)$$

For $P > P^*$, the track is divided into two regions, as defined by the coordinates $x$ and $y$ [Fig. 4(c)]. In the region $0 < x < l$, the track deflection is denoted by $\hat{v}_x$ and the ballast resistance is $\rho(x) = \rho_0 =$ constant; in the region $0 < y < \infty$, the track deflection is denoted by $\hat{v}_y$ and the ballast resistance is represented by a Winkler foundation with modulus $k$. It should be noted that length $l$ is variable and is determined as part of the analysis. The unknown length will depend on the load $P$, such that $l = 0$ when $P = P^*$ and $l$ increases as $P$ increases.

The simplified track equations governing the two regions are

$$2EI\hat{v}_x'''' - \kappa\hat{v}_x'' + \rho_0 = 0 \quad 0 \le x \le l \quad (55)$$

$$2EI\hat{v}_y'''' - \kappa\hat{v}_y'' + k\hat{v}_y = 0 \quad 0 \le y \le \infty \quad (56)$$

rewritten

$$\hat{v}_x'''' - \bar{\beta}^2\hat{v}_x'' = \frac{-\rho_0}{2EI} \quad 0 \le x \le l \quad (57)$$

$$\hat{v}_y'''' - \bar{\beta}^2\hat{v}_y'' + \alpha\hat{v}_y = 0 \quad 0 \le y \le \infty \quad (58)$$

These two fourth-order equations require nine boundary and matching conditions to determine the eight integration constants and the as yet unknown length $l$. They are

$$\hat{v}_x'(0) = 0; \quad \hat{v}_x'''(0) = \frac{P}{4EI}; \quad \hat{v}_x(l) = \hat{v}_y(0) \quad (59-61)$$

$$\hat{v}_x'(l) = \hat{v}_y'(0); \quad \hat{v}_x''(l) = \hat{v}_y''(0); \quad \hat{v}_x'''(l) = \hat{v}_y'''(0) \quad (62-64)$$

$$\hat{v}_y(0) = \hat{v}^* = \frac{\rho_0}{k}; \quad \lim_{x\to\infty} \{\hat{v}_y, \hat{v}_y'\} \to \text{finite} \quad (65, 66)$$

Eq. (57) is a fourth-order, nonhomogeneous equation with constant coefficients; the general solution to the equation is

$$\hat{v}_x(x) = a_1 \cosh \bar{\beta}x + a_2 \sinh \bar{\beta}x + a_3x + a_4 + \frac{\rho_0x^2}{4EI\bar{\beta}^2} \quad (67)$$

The solution to (58) is (50), rewritten as

$$\hat{v}_y = e^{-\xi y}(b_1 \cos \eta y + b_2 \sin \eta y) + e^{\xi y}(b_3 \cos \eta y + b_4 \sin \eta y) \quad (68)$$

where $\bar{\beta}$ is defined in (39) and $\xi$ and $\eta$ are defined in (51). Substituting (67) and (68) into (59)–(61) and (63)–(66), yields the eight integration constants

$$a_1 = \frac{-1}{4EI\Delta}\left\{\frac{4\rho_0\psi}{\bar{\beta}^4} + \frac{P\tilde{\Delta}}{\bar{\beta}^3}\right\}; \quad a_2 = \frac{P}{4EI\bar{\beta}^3}; \quad a_3 = \frac{-P}{4EI\bar{\beta}^2} \quad (69-71)$$

$$a_4 = \frac{1}{4EI\Delta}\left\{\frac{\rho_0}{2\lambda^4}[\Delta(1 - 2\psi^2(\bar{\beta}l)^2) + 8\psi^3 \cosh \bar{\beta}l] + \frac{P}{\bar{\beta}^3}[\bar{\beta}l\Delta + \sqrt{4\psi + 1}]\right\} \quad (72)$$

$$b_1 = \hat{v}^* \quad (73)$$

$$b_2 = \frac{1}{2EI\Delta\sqrt{4\psi - 1}}\left\{\frac{\rho_0}{4\lambda^4}[\sqrt{4\psi + 1}(1 - 2\psi)\cosh \bar{\beta}l + (1 - 8\psi^2)\sinh \bar{\beta}l] + \frac{P}{\bar{\beta}^3}\right\} \quad (74)$$

$$b_3 = 0; \quad b_4 = 0 \quad (75)$$

in which $\psi = \lambda^2/\bar{\beta}^2$ and

$$\Delta = (2\psi + 1)\cosh \bar{\beta}l + \sqrt{4\psi + 1} \sinh \bar{\beta}l \quad (76)$$

$$\tilde{\Delta} = (2\psi + 1)\sinh \bar{\beta}l + \sqrt{4\psi + 1} \cosh \bar{\beta}l \quad (77)$$

The final matching condition, (62), is used to determine the unknown length $l$. Substituting (67) and (68) into (62) and simplifying the result yields

$$2\psi\frac{P\bar{\beta}}{\rho_0} + \left\{\frac{1}{\psi}\sqrt{4\psi + 1} + \left[2(\bar{\beta}l) - \frac{P\bar{\beta}}{\rho_0}\right](2\psi + 1)\right\} \cosh \bar{\beta}l + \left\{\frac{1}{\psi}(2\psi + 1) - 4\psi + \left[2(\bar{\beta}l) - \frac{P\bar{\beta}}{\rho_0}\right]\sqrt{4\psi + 1}\right\} \sinh \bar{\beta}l = 0 \quad (78)$$

Eq. (78) is a nonlinear algebraic equation in the nondimensional length parameter $\bar{\beta}l$. It depends only on the parameters $P\bar{\beta}/\rho_0$ and $\psi$. Eq. (78) was solved numerically for $\bar{\beta}l$ for a range of values for $P\bar{\beta}/\rho_0$ and $\psi$. Results are presented in Fig. 6. With the length $l$ determined, the solution is complete.

Eq. (67) and (68) are closed-form expressions for the deformation, and with appropriate derivatives the internal member forces, of the track structure as functions of the geometric and material properties of the track and ballast. In this case, however, the analysis is valid for deformations in which the ballast response is nonlinear. The maximum deflection, at $x = 0$, is given by

$$\hat{v}_x(0) = a_1 + a_4 \quad (79)$$

and the maximum bending moment in the two rails, at $x = 0$, is given by

$$M_b(0) = -2EI\left\{\bar{\beta}^2a_1 + \frac{\rho_0}{2EI\bar{\beta}^2}\right\} \quad (80)$$

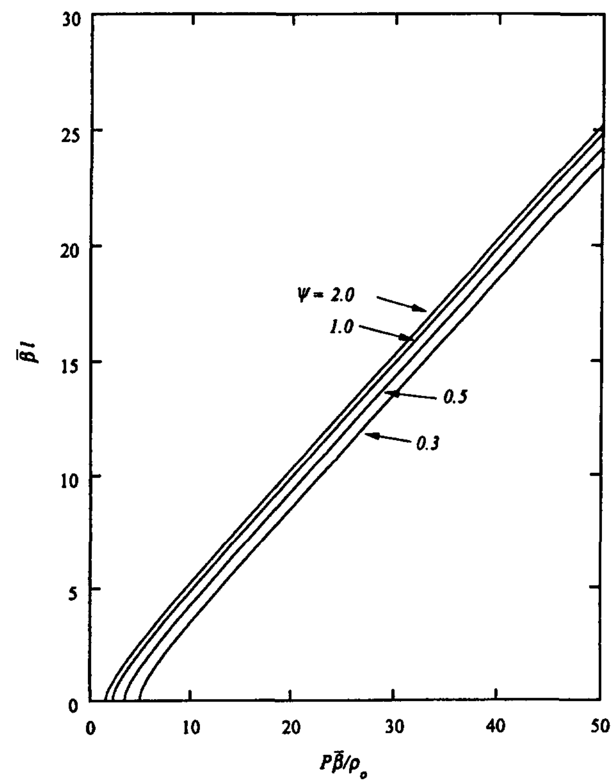


**FIG. 6. Determination of Length $l$**





J. Transp. Eng., 1997, 123(3): 202-208

## DETERMINATION OF TRACK PARAMETERS AND COMPARISON OF ANALYTICAL AND EXPERIMENTAL RESULTS

In addition to the standard track parameters, $E$, $I$, $E_0$, $I_0$, $a$, and $h$, values for $k$, $\hat{v}^*$, $\rho_0$, and $s$ are needed to conduct an analysis of the track response. If these properties are known for a section of track that is similar in design and construction to the analyzed track, these may be used in the calculations; otherwise, values must be determined using a more direct approach. One approach would be to conduct one test to determine the rotational stiffness $s$ of a fastener, and another test of a rigid track in ballast to measure the ballast parameters $k$, $\rho$, and $\hat{v}^*$. The alternative is to infer the parameters from load-deflection data of a tested track. A method for determining the parameters using the latter approach is proposed herein that is based on a least-squares fit to load-deflection test data.

Assume that lateral load-deflection data is obtained for the section of track to be analyzed, or for a section of track of similar design and construction. Deflections are recorded at the point of application of the load and measurements are taken at several load increments. It is assumed that the load is applied well into the nonlinear regime of the ballast response. Thus, corresponding to each load level $P_i$, there exists a measured deflection $\hat{v}_i$. With this information, a load versus deflection-at-the-load curve is constructed, like the one shown in Fig. 7. Using this data, and the simplified equations for deflection at $x = 0$ [(53) evaluated at $x = 0$ and (79)], a trial and error procedure is used to determine the parameters that minimize the squared error between the analytical and experimental results.

The least-squares method is implemented as follows. Values for $\hat{v}^*$, $k$ and $s$ are assumed, from which are computed $\rho_0 = k\hat{v}^*$ and $P^*$. Deflections [denoted as $\hat{v}_x(0)|_{P=P_i} = \hat{v}_{x_i}$] are then computed for each experimental load $P_i$, using (53) if $P_i < P^*$, and using (79) if $P_i > P^*$. Finally, the sum of the squared errors between the analytical predictions and experimental data is computed for the assumed track parameters, i.e.,

$$R^2 = \sum_{i=1}^{n} (\hat{v}_{x_i}^2 - v_i^2) \tag{81}$$

where $n$ = number of experimental data points. The procedure can be implemented in a simple computer program that searches for the best fit within a range of reasonable values for the three track parameters. The values $k$, $\hat{v}^*$, and $s$ that minimize $R^2$ are the final track parameters.

To illustrate the procedure in an actual problem, parameters

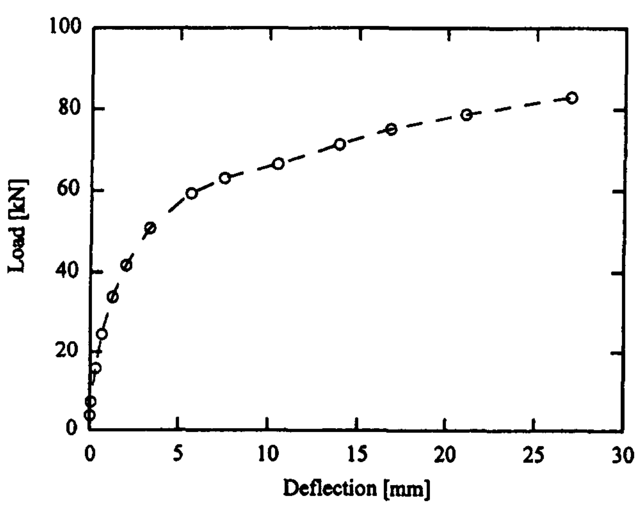


**FIG. 7. Experimental Load-Deflection Data [from Choros et al. (1980)]**

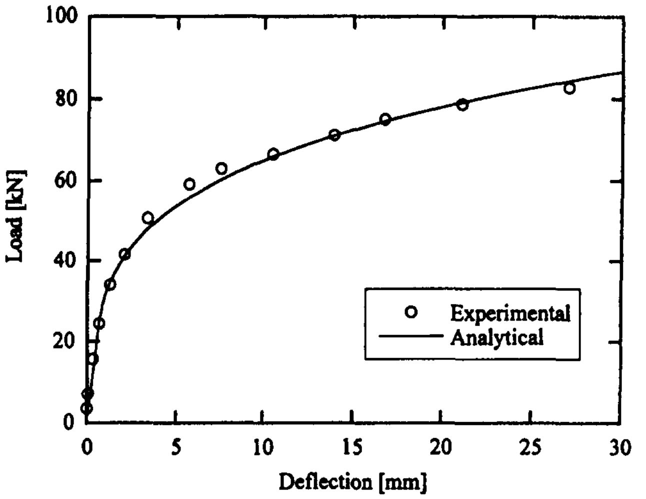


**FIG. 8. Comparison of Analytical and Experimental Results with $k$ = 22,500 kN/m² (3.26 ksi), $\hat{v}^*$ = 0.066 cm (0.025 in.) and $s$ = 9.8 kN-m/rad (87 kip-in./rad), and $\rho_0$ = 0.15 kN/cm (0.085 kip/in.) [Experimental Data from Choros et al. (1980)]**

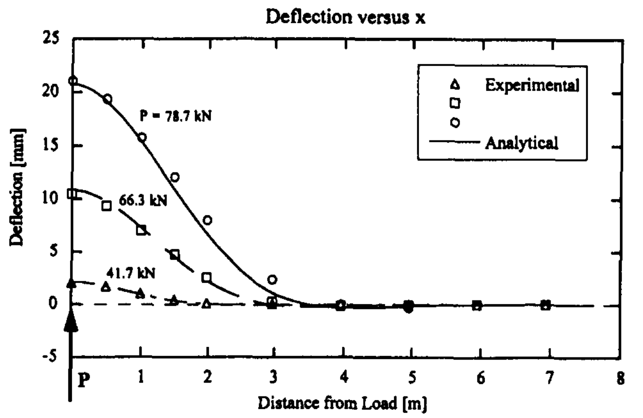


**FIG. 9. Comparison of Analytical and Experimental Deflection Profiles with $k$ = 22,500 kN/m² (3.26 ksi), $\hat{v}^*$ = 0.066 cm (0.025 in.) and $s$ = 9.8 kN-m/rad (87 kip-in./rad), and $\rho_0$ = 0.15 kN/cm (0.085 kip/in.) [Experimental Data from Choros et al. (1980)]**

were determined from the test data shown in Fig. 7. The track, which was tested at the Association of American Railroad's Track Laboratory, in Chicago, Illinois (Choros et al. 1980), was constructed of 136 RE Rails, 177 mm by 228 mm (7 in. by 9 in.) wooden ties spaced at 495 mm (19.5 in.) on center, and cut spike fasteners. The ballast consisted of No. 4 AREA limestone, 304 mm (12 in.) deep with 304 mm (12 in.) shoulders, on top of a 152 mm (6 in.) limestone subballast. The track has the following properties: $E = 206 \times 10^6$ kN/m² ($30 \times 10^3$ ksi), $I = 6.04 \times 10^{-6}$ m⁴ (14.5 in.⁴), $E_0 = 9.8 \times 10^6$ kN/m² ($1.42 \times 10^3$ ksi), $I_0 = 1.77 \times 10^{-4}$ m⁴ (425 in.⁴), $a$ = 0.5 m (19.5 in.), and $h$ = 1.51 m (59.4 in.).

The least-squares procedure was implemented as described previously. The parameters that best fit the load-deflection data for the track were determined to be $k$ = 22,500 kN/m² (3.26 ksi), $\hat{v}^*$ = 0.066 cm (0.025 in.), and $s$ = 9.8 kN-m/rad (87 kip-in./rad). This yields a value $\rho_0$ = 0.15 kN/cm (0.085 kip/in.). The value obtained for $s$ is fairly low, as one would expect for a track with cut spike fasteners.

Fig. 8 presents a comparison between the experimental data and the analytical results, with the track parameters previously determined. The solid line represents the analytical results, the circular points the experimental data. Note that the analytical results agree extremely well with the experimental data, over the entire load range. Presented in Fig. 9 is a comparison between the analytical and experimental deflection profiles.



J. Transp. Eng., 1997, 123(3): 202-208

Again, the solid lines correspond to the analytical solution and the discrete points, the experimental deflections (at different tie locations). Once again, the analytical solution is in close agreement with the experimental data, over the entire length of the track, and for various load levels.

## CONCLUSIONS

An analysis of a crosstie track in the lateral plane has been presented that is based on the new track equations derived by Kerr and Zarembski (1981a). Closed-form solutions were obtained for the exact and simplified new track equations, when the ballast resistance was modeled as a linear Winkler foundation with modulus $k$. Results of the two linear analyses were compared and shown to be in good agreement, thus justifying the use of the simplified equations. A closed-form solution was also obtained for the track deflection using the simplified equations and a bilinear approximation to the nonlinear ballast resistance. The resulting solutions have well defined coefficients in terms of the geometric and material properties of the rails, ties, rail-tie fasteners and ballast. A method for calculating the corresponding track parameters was presented that is based on a least-squares fit to experimental load-deflection data. Finally, a comparison between the analytical and experimental results showed good agreement over the full range of loads and over the entire length of track.

The results presented should be useful for designers of crosstie railroad tracks. The solutions represent a significant advance over the traditional analysis, which ignores the contribution of the ties and rail-tie fasteners to the bending stiffness of the track, and the nonlinearity of the ballast resistance. The results may be used to easily compare different design alternatives, which should result in improved and more economical designs. Finally, the solutions may be used to conduct parametric studies to determine the effect of varying track parameters on the deformation and stress of the track.

## ACKNOWLEDGMENTS

The writer would like to acknowledge Timothy Elliott, a student at the University of Delaware, for developing the computer programs used in this study. The writer would also like to acknowledge Professor Arnold Kerr of the University of Delaware for his valuable comments and for reviewing the manuscript.

## APPENDIX I. REFERENCES

Arbabi, F., and Li, F. (1988). "Effect of nonlinear parameters on stresses in railroad tracks." *J. Struct. Engrg.*, ASCE, 114(1), 165–183.

Beyer, W. H., ed. (1981). *CRC standard mathematical tables*. CRC Press, Inc., Boca Raton, Fla.

Choros, J., Zarembski, A. M., and Gitlin, I. (1980). "Laboratory investigation of lateral track shift." *Res. Rep. FRA/ORD-80/27*, Fed. Railroad Admin., Washington, D.C.

Dogneton, P. (1978). "The experimental determination of the axial and lateral track-ballast resistance." *Railroad Track Mechanics and Technology; Proc., Symp.*, A. D. Kerr, ed., Pergamon Press, Inc., Tarrytown, N.Y.

Kerr, A. D., and Accorsi, M. L. (1985). "Generalization of the equations for frame-type structures; a variational approach." *Acta Mechanica*, 56, 55–73.

Kerr, A. D., and Accorsi, M. L. (1987). "Numerical validation of the new track equations for static problems." *Int. J. Mech. Sci.*, 29(1), 15–27.

Kerr, A. D., and El-Sibaie, M. A. (1987a). "On the new equations for the lateral dynamics of a rail-tie structure." *J. Dyn. Sys., Measurement and Control; Trans. ASME*, 109(2), 180–185.

Kerr, A. D., and El-Sibaie, M. A. (1987b). "Validation of new equations for dynamic analysis of tall frame-type structures." *Earthquake Engrg. and Struct. Dyn.*, 15(5), 549–563.

Kerr, A. D., and Zarembski, A. M. (1981a). "The response equations for a cross-tie track." *Acta Mechanica*, 40, 253–276.

Kerr, A. D., and Zarembski, A. M. (1981b). "On the new equations for the cross-tie track response in the lateral plane." *Res. Rep. CE-81-18*, Dept. of Civ. Engrg., Univ. of Delaware, Newark, Del.

## APPENDIX II. NOTATION

*The following symbols are used in this paper:*

$A$ = cross-sectional area of single rail;
$a$ = rail tie spacing;
$E$ = Young's modulus of rail steel;
$E_0$ = Young's modulus of ties;
$h$ = track gauge;
$I$ = moment of inertia of single rail about its vertical centroidal axis;
$I_0$ = moment of inertia of a tie about its vertical centroidal axis;
$K^*$ = track parameter that is function of flexural rigidity of tie, tie spacing, and track gauge;
$k$ = initial linear stiffness in ballast resistance function;
$\hat{M}$ = total bending moment in track beam;
$\tilde{M}$ = bending moment due to $\tilde{N}$;
$M_b$ = bending moment in two rails;
$\hat{N}$ = axial force of track beam;
$\tilde{N}$ = axial force in rail due to lateral bending;
$P$ = lateral load;
$P^*$ = lateral load at which the displacements are no longer linear;
$s$ = rotational stiffness of single rail-tie fastener;
$s^*$ = rotational stiffness divided by tie spacing;
$\hat{u}$ = axial displacement of track axis;
$\tilde{V}$ = shear force in two rails;
$\hat{v}$ = lateral displacement of track axis;
$\hat{v}^*$ = transition displacement in ballast resistance function;
$\kappa$ = track parameter which is function of $K^*$ and $s^*$; and
$\rho_0$ = constant ballast resistance.



J. Transp. Eng., 1997, 123(3): 202-208